for Handbook on "Solid-State Photoemission and Related methods: Theory and Experiment",
W. Schattke and M.A. Van Hove, eds.

Chapter 2
Overview of Surface Structures

M.A. Van Hove

Materials Sciences Division and Advanced Light Source,
Lawrence Berkeley Laboratory,
Berkeley, CA 94720, USA

and

Department of Physics
University of California at Davis
Davis, CA 95616, USA

Abstract

The atomic-scale structure of a surface is fundamental to understanding its various properties, be they electronic, magnetic, optical, chemical, or tribological. This chapter surveys the current state of knowledge of surface structure, and includes a discussion of the main methods employed to determine surface structure.

2.1 Introduction

Surface science [1,2] has enabled the detailed structural determination of a large number of well-prepared surfaces since about 1970 [3]. A wide variety of materials has been studied, with particular emphasis on metals and semiconductors of interest for understanding catalysis and electronic devices, respectively.

Ultra-high vacuum techniques have made it possible to control the composition and condition of interfaces at the atomic level, and to determine their structure by using electrons, photons, ions and other probes. Atomically clean crystalline surfaces can be prepared, and can serve as substrate for deposition of foreign matter in submonolayer to multilayer amounts, often called "adsorbate". The interface between a substrate and a multilayer film can also be studied structurally, although with greater difficulty.

Surfaces and interfaces are models for the understanding of many phenomena of technological importance, such as those occurring in semiconductor devices, in heterogeneous catalysis, oxidation and corrosion, electrochemistry, friction and wear.

The substrate can be a metal, an alloy, a semiconductor (whether elemental or compound), an insulator, or any other substance that crystallizes. The clean or adsorbate-covered substrate surface can "reconstruct" into a lattice that is quite different from the three-dimensional bulk lattice, a very characteristic phenomenon of surfaces.

Many types of adsorbate can be deposited on a substrate. Typically, one deposits molecules, resulting frequently in atomic adsorbates due to molecular decomposition, or resulting in adsorbed molecular species directly related to or different from the initial molecule. Atoms or clusters can also be deposited, sometimes in ionic form. Deposition of metals often forms metallic films. Chemisorption occurs when strong substrate-adsorbate bonds form. Otherwise physisorption can occur (at low enough temperatures).

Submonolayer adsorbates often do not order into a lattice, but remain disordered, or else they may create two-dimensionally ordered superlattices; they may also generate close-packed islands. Multilayers can grow into thin films that may be epitaxial, i.e. grow in some orientational coincidence with the substrate lattice, or that may be pseudomorphic, i.e. have periodic crystalline coincidence with the substrate.

2.2 Techniques of surface structure determination

Since about 1970, many methods have been developed and applied to determine the atomic-scale structure of surfaces and interfaces [4]. We will here focus on those methods that are capable of finding atomic positions within about 0.1 Å (0.01 nm). The following list gives the acronyms and full names of many of these techniques:

AD - atomic diffraction
AED - Auger electron diffraction
ARPEFS - angle-resolved photoelectron emission fine structure
ARUPS- angle-resolved ultraviolet photoemission spectroscopy
ARXPD - angle-resolved x-ray photoelectron diffraction
GIXS - grazing-incidence x-ray scattering
HEIS - high-energy ion scattering
HREELS - high-resolution electron energy loss spectroscopy
ICISS - impact-collision ion scattering spectroscopy
IS - ion scattering
ISS - ion scattering spectroscopy
LEED - low-energy electron diffraction
LEIS - low-energy ion scattering
LEPD - low-energy positron diffraction
MEED - medium-energy electron diffraction

MEIS - medium-energy ion scattering
NEXAFS - near-edge x-ray absorption fine structure
PD - photoelectron diffraction
PED - photoelectron diffraction
RBS – Rutherford backscattering
RHEED - reflection high-energy electron diffraction
SEELFS - surface extended-energy-loss fine structure
SEXAFS - surface extended x-ray absorption fine structure
STM - scanning tunneling microscopy
TED - transmission electron diffraction
TOF-SARS - time-of-flight scattering and recoiling spectrometry
XAFS - x-ray absorption fine structure
XANES - x-ray absorption near-edge spectroscopy
XRD - x-ray diffraction
XSW - x-ray standing waves

In this list, the same technique may appear under different acronyms or names. An example is photoelectron diffraction, which appears as ARPEFS, ARUPS, ARXPD, PD and PED. Another example is ion scattering: HEIS, ICISS, IS, ISS, LEIS, MEIS and RBS. The different names often reflect different conditions or parameter ranges, such as ultraviolet light (ARUPS) vs. x-rays (ARXPS), or low (LEED, LEIS), medium (MEED, MEIS) vs. high (RHEED, HEIS) energies.

Figure 1 graphs the number of structures determined by those techniques that have produced detailed and complete structures up through the year 2000 [3]. It illustrates the predominance of LEED in surface structure determination, followed by photoelectron diffraction (in its various forms) and ion scattering (in its various forms).

Figure 1 near here.

Figure 2 breaks down the relative contribution from the different techniques on a yearly basis [from ref. 3]. This graph shows that LEED was the only technique in use until about 1978 and that it has continued to produce more than 50% of determinations since then. At that time, several techniques using synchrotron radiation became available, including prominently photoelectron diffraction, as well as ion scattering, which relies on ion accelerators.

Figure 2 near here.

In the next few sections, we will briefly describe groups of techniques, according to their basic mechanism: diffraction, (non-diffractive) scattering, etc.

Then, we will discuss ordering principles at surfaces, which are responsible for the periodic crystallinity of most of the solved structures. Next we will address the types of surface structure that have been solved, grouped according to types of surfaces, and discuss the kinds of structures that have been found to occur: reconstructions, adsorption of atoms and molecules as overlayers, penetration of adatoms into surfaces, etc.

2.2.1 Diffraction techniques

Diffraction has been a most successful approach to atomic-scale structure determination of bulk materials and surfaces. Diffraction can deliver atomic coordinates at surfaces with precisions in the range of 0.01 to 0.1 Å. LEED, PED and XRD are the main diffraction techniques which have been applied to surface structure determination.

The majority of known surface structures has been studied with low-energy electron diffraction (LEED) [5,6]. LEED uses as probes elastically diffracted electrons with energies in the 20-300 eV range, which corresponds to electron wavelengths in the 0.5-2 Å range. Mono-energetic electrons are beamed at a surface, from which they are diffracted (only elastically scattered electrons are normally recorded). Inelastic scattering processes severely limit the penetration depth of such electrons into a surface to about 5-10 Å, giving a surface sensitivity of only a few atomic layers.

Interferences between different scattering paths pick up the local surface structure information in the form of modulations of diffracted electron beam currents. Elastic interactions are strong enough that multiple scattering of electrons from one atom to another is important in this energy range. This complicates the analysis of experimental diffraction data, but the necessary theoretical methods have been very successful in obtaining bond lengths and angles at surfaces of almost any chemical composition (hydrogen atoms being the major exception).

The methods employed to analyze LEED measurements simulate the entire multiple scattering process in a way similar to the calculation of electronic band structures in the bulk and at the surface. An important part of the process is the fitting of atomic positions to reproduce experimental diffraction data.

X-ray diffraction, with its inherent conceptual simplicity, has been an obvious choice for surface crystallography [7]. However, long mean free paths of x-rays in solids permit the desired surface sensitivity only when grazing incidence and/or emergence are used: angles within a fraction of a degree from the surface plane are required. This demands extremely flat surfaces and strict control of diffraction angles, both challenging experimental tasks. Also a sufficient photon flux is required, which is often sought at synchrotron radiation facilities. In fact, the relative impact of XRD has grown with the increased availability of synchrotron radiation.

A variant of x-ray diffraction has been applied to obtain interlayer spacings between adsorbates and bulk atomic planes. These bulk atomic planes include not only the planes parallel to the surface, but also any crystallographic planes inclined to the surface. Then "triangulation" allows the

adsorption site to be determined. This approach uses x-ray standing waves due to reflection from atomic planes in the crystal bulk [8]. This method is used in conjunction with detection of the fluorescence that is unique to the adsorbate. The fluorescence is sensitive to interference between the directly reflected beams and beams reflected from the bulk planes; hence it can tell the interplanar separation.

A number of diffraction techniques use internal localized point sources of electrons, instead of external beams. In the case of photoelectron diffraction [9,10,11], electrons are photoemitted from particular electronic orbitals, such as core levels in individual surface atoms. Often synchrotron radiation is used as a source of photons. Those electrons scattered from nearby atoms toward the detector interfere with electrons traveling directly from the emitting atom to the detector, in a way that depends on the local geometry. The electrons are emitted with kinetic energies up to a few thousand eV, where single-scattering events dominate to give a qualitatively simple scattering picture (but multiple scattering must be taken into account for accuracy).

Another point-source diffraction technique is x-ray absorption fine structure (XAFS) [12,13,14,15]. Again, photoelectrons are excited and allowed to scatter from nearby surface atoms. However, in this case the electrons return to the emitting atom and modulate (by wave interference) the emission process itself. This modulation is again interpreted in terms of the local geometry. SEXAFS (surface extended XAFS) uses electron kinetic energies of the order of 1000 eV, and a single-scattering model is often adequate to interpret the experimental data. Any emitted particle can be chosen for detection, including photons, electrons and ions.

Closely related to SEXAFS is near-edge x-ray absorption fine structure (NEXAFS, also called XANES) [14]. NEXAFS is SEXAFS conducted at much lower electron kinetic energies, where multiple scattering is strong. This technique is primarily used to monitor excitations among valence electrons, from which structural information like molecular orientation and bond lengths is accessible. And the polarization of the incident photons can be used to detect the orientation of bonds and thus the orientation of molecules relative to the surface plane, for example.

Another approach uses "electron holography" [16,17,10]. The angular distribution of an emitted electron (e.g. a photoelectron) can be viewed not only as a diffraction pattern to be fit, but also as a hologram to be inverted: such a pattern or hologram is due to interference between the directly emitted wave and the same wave scattered from nearby atoms, in analogy with optical holography. From this hologram, one can computationally reconstruct an image of the neighborhood of the emitting atom, by a Fourier-transform-like inversion. The result is a map that approximates the positions of atoms: each atom in principle is represented by a maximum in this three-dimensional map. The method suffers however from distortions due to electron scattering phase shifts and multiple scattering effects. But it has been found that including holograms taken at multiple energies, together with energy-dependent phases, can appreciably improve the quality of the resulting map. This approach is not guaranteed to work in all cases, but when it does work it saves much effort in solving a structure. Typically, after holographic inversion, a more standard fitting is performed to fine-tune atomic positions.

2.2.2 Scattering techniques

A number of techniques rely on scattering, as opposed to diffraction (interference), to obtain geometrical information from surfaces. Of particular value has been ion scattering both at low energies (around 1 keV) [18,19] and at medium and high energies (100-1000 keV) [20].

Low-energy ions cast wide shadows behind surface atoms. These shadows obscure further atoms if they lie within the shadow cone. By varying the incidence direction, the shadow cone can be swept through the surface and expose or hide individual atoms. It is possible to monitor the disappearance and emergence of atoms in the shadow cone, thereby obtaining structural information. This information tends to be restricted to the top one or two atomic layers, since the shadows obscure all deeper layers. The technique is generally called LEIS (low-energy ion scattering) [18]. Alkali ions provide particularly good structural sensitivity when monitored near the 180º scattering direction: this feature is used in ALICISS (alkali-ion impact collision ion scattering spectroscopy) [21].

Medium- and high-energy ions (helium nuclei and protons are commonly used) are directed along bulk crystal axes of the surface material. The ions can channel relatively deeply into the crystal between rows of atoms, because the shadow cones are in this case very narrow. But if surface atoms deviate from the ideal bulk lattice positions and block the channels through which the ions move, the ions will scatter strongly back out of the surface. This conceptually simple approach has been used successfully to obtain detailed structural information for a number of clean and adatom-covered surfaces. It is uniquely suited to study buried solid-solid interfaces (i.e. interfaces that lie deep in the bulk below a surface), since the ions can be made to penetrate relatively deeply into a surface. The technique still requires ultra-high vacuum for its operation, because the ion beams can only be formed in such a vacuum [22]. Depending on the energy range used, and other experimental choices, the technique is known under the names of medium-energy ion scattering (MEIS) or high-energy ion scattering (HEIS).

2.2.3 Microscopic and topographic techniques

A number of powerful techniques have been developed that study surfaces in a microscopic sense: they image directly individual microscopic parts of a surface rather than structure as averaged over macroscopic distances. Some, like field-ion microscopy (FIM) [23,24] and scanning tunneling microscopy (STM) [25,26] can image individual atoms.

However, none of these microscopic techniques readily provides complete information about bond lengths or other bonding details (unless a close comparison with theory is made). In special conditions, distances parallel to the surface can be obtained with some accuracy, but mostly these techniques are used to map out surface topography or composition, down to atomic resolution in the case of STM and FIM.

2.3 Two-dimensional ordering

Deposition of adsorbates on a single-crystal substrate can produce quite different two-dimensional periodicities than the clean surface has. And the clean surface may have a different two-dimensional periodicity than one would expect from simple truncation of the three-dimensional bulk lattice. We shall in this section first address the question of how ordering takes place at surfaces, with emphasis on the case of adsorbates. Then we shall introduce the main nomenclature that is used in surface science to describe ordered surface structures, whether due to adsorbates or due to reconstructions.

2.3.1 Ordering principles at surfaces

A large number of ordered surface structures can be produced experimentally on single-crystal surfaces, especially with adsorbates [27]. Ordering can manifest itself both as commensurate and as incommensurate structures. There are also many disordered surfaces.

We shall here adopt the following common definitions of the terms coverage and monolayer (however, one should be aware that other definitions are also often used). The surface coverage will be unity when each two-dimensional surface unit cell of the unreconstructed substrate is occupied by one adsorbate (the adsorbate may be an atom or a molecule). A coverage of 1/2 per cell thus corresponds to filling every other equivalent adsorption site. The term monolayer will here indicate a saturated single adsorbate layer with a thickness equal to the dimension of the adsorbate perpendicular to the surface. Thus, deposition after this coverage can only be achieved by starting a second monolayer growing on top of the first monolayer.

The driving force for surface ordering originates, analogous to three-dimensional crystal formation, in the interactions between atoms, ions, or molecules in the surface region. The physical origin of the forces is of various types (covalent, ionic, Van der Waals), and the spatial dependence of these interaction forces is often complex.

For adsorbates, an important distinction must be made between adsorbate-substrate and adsorbate-adsorbate interactions. The adsorbate-substrate interaction is due to strong covalent or ionic chemical forces in the case of chemisorption, or to weak Van der Waals forces in the case of physisorption. Adsorbate-adsorbate interactions may also be of different kinds: they may be strong covalent bonding interactions (as with dense metallic layers), weaker orbital-overlapping interactions or electrostatic interactions (e.g. dipole-dipole interactions), or weak Van der Waals interactions, etc. These are many-body interactions that may be attractive or repulsive depending on the system.

Frequently, an adsorbate lattice is formed that is simply related to the substrate lattice. In the ordered case this yields commensurate superlattices. The most common of these are simple superlattices with one adsorbate per superlattice unit cell. They occur for adsorbate coverages of 1/4, 1/3 or 1/2 per cell, for example. An incommensurate relationship exists when there is no common periodicity between an overlayer and the substrate. Such a structure is dominated by

adsorbate-adsorbate interactions rather than by adsorbate-substrate interactions. The classic example is that of rare-gas monolayers physisorbed (weakly adsorbed) on almost any substrate.

2.3.2 Nomenclature

Single-crystal surfaces are characterized by a set of Miller indices that indicate the particular crystallographic orientation of the surface plane relative to the bulk lattice. Thus, surfaces are labeled in the same way that atomic planes are labeled in x-ray crystallography. For example, a Pt(111) surface exposes a hexagonally close-packed layer of atoms, given that platinum has a face-centered cubic bulk lattice. For reference, such a surface is often additionally labeled (1x1), thus Pt(111)-(1x1): this notation indicates that the surface is not reconstructed or otherwise modified into a periodicity different from that expected from simple truncation of the bulk lattice.

Most surfaces exhibit a different two-dimensional periodicity than expected from the bulk lattice, as is most readily seen in diffraction patterns: often additional diffraction features appear which are indicative of a "superlattice". This corresponds to the formation of a new two-dimensional lattice on the surface, usually with some simple relationship to the expected "ideal" (1x1) lattice. For instance a layer of adsorbate atoms may occupy only every other equivalent adsorption site on the surface, in both surface dimensions. Such a lattice can be labeled (2x2): in both surface dimensions the repeat distance is doubled relative to the ideal substrate.

In general, the (2x2) notation can take the form (mxn)Rα°, called Wood notation (Wood, 1964). Here the numbers m and n are two independent stretch factors in different surface directions. These numbers need not be integers: irrational values yield incommensurate lattices, while rational values, expressible as an integer or as a ratio of integers, correspond to commensurate lattices. In addition, this stretched unit cell can be rotated by any angle α° about the surface normal. Thus, the Wood notation allows the (1x1) unit cell to be stretched and rotated; however, it conserves the angle between the two unit cell vectors in the plane of the surface, disallowing "sheared" unit cells.

A more general notation is available for all unit cells, including those that are sheared, so that the superlattice unit cell can take on any shape, size and orientation. It is the matrix notation, defined as follows (Van Hove et al, 1986a). We connect the unit cell vectors **a'** and **b'** of the superlattice to the unit cell vectors **a** and **b** of the substrate by the general relations:

$$\mathbf{a}' = m_{11}\mathbf{a} + m_{12}\mathbf{b},$$
$$\mathbf{b}' = m_{21}\mathbf{a} + m_{22}\mathbf{b},$$

The coefficients m_{ij} define the matrix

$$\mathbf{M} = \begin{pmatrix} m_{11} & m_{12} \\ m_{21} & m_{22} \end{pmatrix},$$

which serves to denote the superlattice. The (1x1) substrate lattice and the (2x2) superlattice are then denoted by the matrices

$$\mathbf{M} = \begin{pmatrix} 1 & 0 \\ 0 & 1 \end{pmatrix}$$

and

$$\mathbf{M} = \begin{pmatrix} 2 & 0 \\ 0 & 2 \end{pmatrix},$$

respectively.

2.4 Clean surfaces

Once a clean surface has been prepared, it is often found to have the two-dimensional periodicity which one would expect from simple ideal truncation of the bulk lattice parallel to the surface plane. However, there are many exceptions: they are often called reconstructions and we shall define them to be those clean structures that involve relatively large atomic displacements from an ideally-terminated bulk structure, including in particular the breaking of remaining bonds and/or the making of new bonds. In all cases, whether reconstructed or not, there is the possibility that bond lengths and interlayer spacings near the surface can differ from those in the bulk: this is usually called "surface relaxation".

Figure 3 gives an idea of the types of substrate for which the surface structure has been solved (combining clean and adsorbate-covered surfaces). Notable is the preponderance of non-reconstructed elemental metal surfaces. A good number of reconstructed semiconductor surfaces is also included. There are far fewer structures known for surfaces of alloys and other compounds, such as insulators.

Figure 3 near here.

Figure 4 breaks the surface structures down by substrate lattice. This makes clear that most structure determinations were performed for fcc, bcc and hcp metal surfaces, as well as diamond-lattice surfaces (mainly silicon).

Figure 4 near here.

2.4.1 Bulk-like lattice termination

A number of clean surfaces exhibit a bulk termination (with perhaps some minor relaxations which we will discuss in section 4.3). They are then denoted as having a (1x1) surface lattice.

This occurs most prominently with many pure metal surfaces that have low Miller indices, such as fcc(111), fcc(100), fcc(110), bcc(110), bcc(111), hcp(0001) and hcp(10-10). Among the few oxide surfaces which have been studied, the low-index surfaces derived from the bulk NaCl lattice also exhibit a (1x1) lattice, e.g. NiO(100). A number of alloy surfaces (again, few have been studied) also have a bulk-like termination. Some semiconductor compounds also have the (1x1) termination, such as the (110) surface of many III-V and II-VI compounds (GaAs, AlAs, AlP, GaP, GaSb, InAs, InP, InSb, CdTe, ZnS, ZnSe and ZnTe), although they may can involve large atomic displacements (relaxations).

By contrast, the phenomenon of surface premelting has been well documented, at least for certain Pb surfaces, particularly the (110) surface of this fcc metal [28]. Premelting within a few outermost surface layers is observed already some 100 K below the bulk melting temperature of about 600 K.

2.4.2 Stepped surfaces

Well-annealed clean fcc and bcc metal surfaces often exhibit steps between adjacent flat terraces. So-called vicinal surfaces (which are cut somewhat off from a low-Miller-index plane), have regular arrays of such steps. Such steps are found to be mostly of mono-atomic height [2]. This is partly due to the fact that on ideal fcc and bcc surfaces, successive steps are structurally equivalent and multiheight steps are less favorable. On hcp metal surfaces, however, steps are often of double height. The difference is that on most hcp surfaces mono-atomic height steps alternate among two inequivalent structures and can compose a more favorable double-height step. Similarly, steps on many semiconductor surfaces have a two-atom height. Little is known about step structures at bimetallic and other surfaces.

2.4.3 Relaxations

Surface atoms have a highly asymmetrical environment: they have neighbors toward the bulk and in the surface plane, but none outside the surface. This anisotropic environment forces the atoms into new equilibrium positions, relative to the bulk. For clean unreconstructed surfaces, there is generally a contraction of bond lengths between atoms in the top layer and in the second layer under the surface, relative to the bond length in the bulk: the contraction is on the order of a few

percent [3]. This relaxation in the topmost interlayer spacing is larger the more open (or rougher) is the surface, i.e. the fewer neighbors the surface atom has [29]. The closest packed surfaces, such as fcc(111) and fcc(100), show almost no relaxation; there may even be a very slight expansion for metals like Pd and Pt(111). Relatively large inward relaxations occur by contrast at surfaces like fcc(110), with interlayer spacings contracted by about 10%. The contractions are material dependent, Pb(110) showing a particularly large interlayer spacing contraction of 16%, corresponding to a bond length contraction of 3.7% [30].

Relaxations of interlayer spacings occur also deeper than the second layer [29,31]. The amplitudes of these relaxations decay approximately exponentially with depth. At least in metals, it is common to observe alternating contractions and expansions in the interlayer spacings. Typically, one may find, in penetrating the surface, first a contraction, then an expansion, followed by another expansion, and then again a contraction.

Relaxations parallel to the surface are also expected and observed for atoms at step edges [29,31]: they tend to relax sideways toward the upper terrace of which they are a part.

Semiconductor surfaces often present larger relaxation effects than metal surfaces, because there is more room for bond angle changes in the less close-packed semiconductors [32,33]. The bond lengths also appear to change more than they do in metals. For example, in GaAs(110) and a number of similar unreconstructed surfaces of III-V and II-VI compounds, large rotational relaxations occur. Whereas the bulk has tetrahedral angles of 109.5º, some of the bond angles at surface atoms are reduced to 90 ± 4º while others are increased to 120 ± 4º. These changes vary from layer to layer, and decay to the bulk value within a few atomic layers. In these examples, bond lengths change by up to 9%, but more typically by about 5%; both contractions and elongations occur in the same structure. Such effects are due to the rehybridization of atomic orbitals around the surface atoms. At (110) surfaces of III-V compounds, the group III element (anion) rehybridizes toward sp^2 and a planar neighborhood with 120º bond angles, whereas the group V element (cation) adopts a distorted p^3 hybridization that favors 90º bond angles.

2.4.4 Reconstruction

Among the clean metal surfaces, nearly a dozen are known to reconstruct. Over 40 clean semiconductor reconstructions have been reported. Numerous reconstructions have also been found for oxides and other compounds. Depending on preparation methods, some of these surfaces can present different superlattices, some of which are metastable. Thus, Si(111) reconstructs readily into a stable (7x7) structure, but can also be prepared as a (2x1) structure, a $(\sqrt{3}x\sqrt{3})R30$º structure and even an unreconstructed (1x1) form, all of which are metastable. Similarly, Ir(100) normally reconstructs into a (1x5) lattice, but can be prepared in a metastable (1x1) structure.

Several types of clean-surface reconstruction can be distinguished [34]. First, one finds displacive reconstructions, in which atoms are displaced slightly from their ideal bulk-like positions in different directions which break the ideal periodicity and create a superlattice. Generally, no bonds

are broken or created in this type of reconstruction, but bond lengths and angles are changed. Mo and W(100) are good examples.

Next are the missing-row reconstructions, exemplified by Ir, Pt and Au(110) [35]. In this case, rows of atoms are missing from the ideally-truncated substrate. This creates narrow facets which are more close-packed than the ideal surface. The most common missing-row reconstruction produces a (2x1) unit cell with facets 2 atoms wide.

Another type of reconstruction seen on metal surfaces is the formation of a closer-packed top layer. Such a reconstruction occurs for Ir, Pt and Au(100), as well as Au(111) [36]. In these cases, the interatomic distance within the topmost layer shrinks by a few percent parallel to the surface. It then becomes more favorable for this layer to collapse into a denser layer that is nearly hexagonally close packed rather than maintain the square lattice of the underlying layers.

Semiconductors often exhibit bond breaking and creation in one or more surface layers, relative to the ideal truncation [32,33]. This effect is due to the directionality of the bonding in these materials. The "dangling" bonds broken by the creation of the surface are energetically unfavorable.

An important driving mechanism for semiconductor reconstruction is the minimization of the number of such dangling bonds. This is accompanied by more or less drastic rearrangements of the surface lattice. A relatively simple case occurs with Si(100), where atom pairing satisfies half of the dangling bonds, forming a (2x1) superlattice. A more extensive rearrangement is found in the (2x1) reconstruction of Si(111) and diamond C(111): here atoms bond in zigzag chains along the surface, while the 6-membered rings of the bulk are replaced by 5- and 7-membered rings next to the surface.

The Si(111)-(7x7) surface is the most complex reconstruction solved to date [37,38]. It incorporates many of the abovementioned effects, and some additional ones. This reconstruction involves 12 "adatoms" per (7x7) unit cell. One half of the unit cell presents a stacking fault between the first and second bilayers, as if the top bilayer had been rotated by 180º about the surface normal. This stacking fault joins the non-faulted half of the unit cell at a seam that consists of paired atoms. Six such seams meet at large and deep holes (one hole per unit cell), which expose the second bilayer. The combination of adatoms, dimers and stacking fault reduces the number of dangling bonds per (7x7) unit cell from 49 on the ideal unreconstructed surface to 19 on the reconstructed surface.

2.4.5 Surface segregation

A number of bulk compounds like oxides, carbides, sulfides and semiconductors maintain their bulk composition at the surface. There are, however, numerous exceptions that exhibit a deviating surface composition. An example is the case of the (111) faces of GaAs, GaP, and other such semiconductors, where a deficiency of Ga leads to a (2x2) reconstruction due to Ga vacancies [39].

The clean metallic alloys fall into two main categories: those for which the bulk alloy is ordered and those for which it is disordered. It appears that the surface structures of ordered bulk alloys are generally also ordered and maintain the bulk concentration. With disordered bulk alloys, the surface is most often also disordered, but surface segregation can be very marked and can be strongly layer-dependent, with the possibility of an oscillating layer-by-layer concentration. Other alloys, exemplified by Cu-rich CuAl [40], are disordered in the bulk, but order at some faces for certain bulk compositions.

2.4.6 Quasicrystals

Certain alloys form so-called quasicrystals: they are mostly ternary alloys with a majority component of Al. Quasicrystals have orientational order but no translational periodicity, and they can exhibit symmetries that are not allowed in periodic crystals, such as 5-, 8-, 10- and 12-fold rotational symmetry.

The surface structure of the 5-fold symmetrical surface of two quasicrystals has been studied: AlPdMn [41] and AlCuFe [42]. The main features are a bulk-like termination of the lattice, exposing an Al-rich layer, with interlayer relaxations similar to those seen of metal surfaces such as fcc(110).

2.5 Adsorbate-covered surfaces

A large number of atomic and molecular adsorbates have been studied on single-crystal surfaces over the last decades [27]. Very different structures are found when physisorption is compared with chemisorption, or when comparing atomic with molecular adsorption, or when mixing in a second type of adsorbate. Such differences will be addressed in this section. We shall also discuss multilayer growth, relaxations, reconstructions, compound formation and surface segregation of surfaces upon adsorption.

Figure 5 compares the numbers of surface structures solved for different adsorption modes. Simple atomic overlayers form the great majority. There are also a good number of molecular adsorbate structures, as well as a series of pseudomorphic ultrathin films (these have a 2-dimensinal lattice that coincide with that of the substrate).

Figure 5 near here.

2.5.1 Physisorption

At low enough temperatures most gas-phase species will physisorb on any surface. Particularly with inert gases and with saturated hydrocarbons, physisorption is commonplace and stable on many types of substrate.

The simpler among the observed LEED patterns for physisorbed species can often be easily interpreted in terms of structural models. The known Van der Waals sizes of the species lead to satisfactory structures which are more or less close-packed. This is especially straightforward with inert gases.

Physisorption allows the formation of multilayers, which normally grow with their own lattice constant on any substrate. For example, xenon films exposing a Xe(111) surface have been grown on an Ir(100) substrate and analyzed by LEED to show that the bulk fcc Xe structure is maintained [43].

2.5.2 Atomic chemisorption sites and bond lengths

Frequently, chemisorbed atoms order well on surfaces, particularly at specific coverages like 0.25, 0.5, 0.75, etc. per cell, where regular superlattices can develop. In many cases, order-disorder transitions are observed as the temperature is raised.

We first consider the adsorption site of chemisorbed atoms. The simple atomic adsorption structures on metal surfaces are generally characterized by the occupancy of high-coordination sites. Thus, Na, S, and Cl overwhelmingly adsorb over "hollows" of the metal surface, bonding to as many metal atoms as possible [3].

The situation is slightly more complicated with the smaller adsorbates, such as H, C, N, and O, on metal surfaces. And all adsorbates appear to behave in a more complex manner on semiconductor surfaces. By contrast, little crystallography has been accomplished on atomic adsorption on other types of substrates, such as insulating compounds and alloys.

With the adsorption of smaller adsorbates, there still remains a preference for high-coordination sites. However, the atoms often penetrate deeper within or even below the first substrate layer. The penetration can be interstitial (as occurs with small atoms on metals) or substitutional (as is relatively more frequent on semiconductors and compounds). In either case the surface can reconstruct as a result, especially at higher coverages. For instance, a monolayer of N penetrates into interstitial octahedral sites between the first two layers of Ti(0001) with minimal distortion of the Ti lattice [44]. Both C and N burrow themselves within the hollow sites of the Ni(100) surfaces so as to be almost coplanar with the topmost Ni atoms [45,46,47]. The nearest Ni atoms are also pushed sideways by perhaps 0.4 Å, a good example of adsorbate-induced reconstruction.

One of the few known structures of an adatom at steps is that of O on Cu(410) [48]. The Cu(410) surface consists of (100) terraces, 3 atoms wide, on which the O adatoms can arrange themselves in a c(2x2) array at hollow sites. Oxygen atoms bond within the step edge between adjacent Cu step

atoms: the bonding arrangement is just like the 4-fold hollow site, except that one of the four surrounding Cu atoms is missing.

Atomic adsorption on semiconductors shows three emerging major trends in the adsorption sites: low-coordination adatoms, high-coordination adatoms, and substitutional atoms.

Some atoms adsorbed on the (111) face of C (diamond), Si and Ge cap the dangling bonds of the ideally truncated surface. For instance, H, Cl, Br and I choose capping sites on Si(111), forming bonds through single coordination to Si atoms. These adatoms in effect continue the bulk Si lattice outward, removing any clean-surface reconstruction when the adatom coverage is large enough.

The second trend is illustrated by several adsorbed atoms on Si(111) and Ge(111) which at low coverage appear to prefer the so-called T_4 adatom site (the same site that Si and Ge adatoms occupy in the clean-surface reconstructions: this site lies above a triangle of substrate atoms, with one other substrate atom just below, resulting in 4 adsorbate-substrate bonds). The adatoms are thereby bonded to 4 substrate atoms of the top bilayer. Examples are Pb on Ge(111) [49], and both Al (50,51) and Ga on Si(111) [52]. It appears from these results that the larger adatoms induce larger distortions in the substrate.

The third trend involves substitutional penetration of the adsorbate into the substrate. One example is boron on Si(111): instead of becoming a T_4 adatom, B interchanges its position with the Si atom immediately below the T_4 site (this substitutional site is called B_5 site) [53]. Another example is Al on GaAs(110), in which Al substitutionally replaces Ga atoms, largely retaining the relaxations of clean GaAs(110) [54].

Next we consider bond lengths between adsorbate and substrate atoms. The observed bond lengths generally fall well within 0.1 Å of corresponding bond lengths measured in bulk compounds and molecules. In a few cases the accuracy is sufficient to detect chemically significant variations in bond lengths. As a dramatic example, when the surface coverage of Cs atoms is varied from 1/3 to 2/3 per cell on Ag(111), the Ag-Cs bond length changes from 3.20 to 3.50 Å [55]. In this case the charging state of the adsorbate changes with coverage (as observed through work function changes), with a concomitant effect on bond lengths. This also illustrates an expected effect of mutual interactions between adsorbates: the denser the adsorbate layer, the weaker the individual adatom-substrate bonds.

2.5.3 Atomic multilayers

Atomic multilayer growth has been studied most frequently for metal deposition on metal surfaces, and for semiconductor or metal deposition on semiconductors [56,57,58]. Also, the growth of oxides and other compounds has been studied, but rarely in structural detail. Two aspects are of particular interest: 1) the growth mode, whether layer-by-layer and/or epitaxial or as three-dimensional crystallites; and 2) the interface structure between the substrate and the growing film. For metals, the growth mode tends to attract the most attention, while the interface structure is of particular interest for growth on semiconductors.

2.5.3.1 METALLIC ADSORPTION ON METALS

At low coverages, most of the metallic adsorbates form commensurate ordered overlayers: the overlayer unit cells are closely related to the substrate unit cells. Furthermore, in many cases a (1x1) LEED pattern is observed. This suggests that these adsorbed metal atoms attract each other to form two-dimensional close-packed islands. On the other hand, a disordered LEED pattern is observed when the adsorbed metal atoms repel each other. This is found for example in the case of alkali metal adsorption on a transition metal, since the charged adatoms undergo repulsive interactions.

Some metals undergo layer-by-layer growth, while others form three-dimensional crystallites ("balls"). Many cases fall between these two extremes. Comparison of the surface tension of the adsorbate metal and of the substrate metal gives a rough and not very reliable guide to these phenomena.

The limit of layer-by-layer growth has been studied in structural detail, thanks to the frequent formation of simple (1x1) overlayer unit cells. Striking is the growth of metastable films with lattices that are not favored in the bulk. Fe grown on Ni(100) [59] and Cu(100) [60] has received considerable attention: the Fe film can be made to grow with an fcc-like lattice (which continues the fcc lattice of Cu), rather than with its bcc bulk lattice. On Ni, the outermost Fe layer tends to relax into a wavy pattern of positions. The spacing between overlayers varies both from layer to layer and, for a given layer, as the film thickness grows, so that the Fe film does not adopt a perfectly cubic lattice; but the Fe is 12-fold coordinated, as in the fcc lattice. Such effects are particularly interesting in view of the magnetic properties of thin metallic films, which appear to depend strongly on the growth geometry.

2.5.3.2 MULTILAYER GROWTH ON SEMICONDUCTORS

Multilayer growth on semiconductor substrates is of great importance to the semiconductor industry: it is highly relevant to the formation and electrical properties of semiconductor-metal contacts, of semiconductor-semiconductor heterojunctions and of "superlattices" (here understood to mean the stacking of thin films of alternating composition). Nevertheless, relatively little structural information on the Ångström level is available. On a more qualitative level, many of the features described above for metal-metal interfaces are thought to apply here as well [58].

One reason for the scarcity of structural information of such interfaces is the difficulty in studying deeply buried interfaces. Even with interfaces buried only a few atomic layers below a solid-vacuum surface, few experimental techniques are capable of sampling the buried structure. The technique which has been most successful in this respect has been high-energy ion scattering (HEIS), while LEED, SEXAFS and LEIS have also contributed by studying shallow buried interfaces.

A few interfaces between Si and a metal silicide have been investigated in detail. Examples are the Si(111)-$NiSi_2$(111) interface [61] and the similar interface produced with Co instead of Ni [62]. In both cases, the two materials match very closely in lattice constant parallel to the interface, forming a (1x1) surface lattice. Despite the identical lattices of $NiSi_2$ and $CoSi_2$, the bonding arrangement across the silicon-silicide interface is topologically slightly different between the two cases.

2.5.4 Molecular adsorption

Well over 400 ordered LEED patterns have been reported for the adsorption of molecules [27]. By far the most frequently studied substrates are metals. Platinum substrates have been most extensively used, due no doubt to their importance in heterogeneous catalysis. The most common adsorbates are CO (carbon monoxide), NO (nitric oxide), C_2H_2 (acetylene), C_2H_4 (ethylene), C_6H_6 (benzene), C_2H_6 (ethane), HCO_2 (acetate), HCOOH (formic acid), and CH_3OH (methanol).

Ordered LEED patterns for organic adsorption are frequent at lower temperatures. They can often be interpreted in terms of close-packed layers of molecules, consistent with known Van der Waals sizes and shapes. These ordered structures usually are commensurate with the substrate lattice, indicating strong chemisorption in preferred sites. It appears that many hydrocarbons lie flat on the surface, using unsaturated π-orbitals to bond to the surface. By contrast, non-hydrocarbon molecules form patterns that indicate a variety of bonding orientations. Thus CO and NO are found to strongly prefer an upright orientation. However, upon heating, unsaturated hydrocarbon adsorbates evolve hydrogen and new species may be formed which bond through the missing hydrogen positions, often in upright positions. An example is ethylidyne, CCH_3, which can be formed from ethylene, C_2H_4, upon heating. Ethylidyne has the ethane geometry (H_3CCH_3), but three hydrogens at one end are replaced by three substrate atoms: the resulting assembly could be denoted M_3CCH_3, where M is a metal atom.

2.5.4.1 MOLECULAR ADSORPTION SITES AND ORDERING

When the adsorbate-substrate bond is strong and localized, the molecule presents clear preferences for particular adsorption sites and it orders well. Thus, ethylidyne (CCH_3) bonds through one carbon atom to a three-fold coordinated hollow site on many fcc(111) surfaces, and typically orders as a (2x2) overlayer [63,64].

When the molecular species is large and bonds to many metal atoms simultaneously, as is the case with benzene lying flat on a surface, there is less preference for particular sites, which then depend on the metal and can easily be affected by coadsorbed species (e.g. acceptors like CO). For instance, benzene will shift its center from a bridge site to a hollow site when coadsorbed with CO on Rh(111). Ordering is relatively weak under such conditions. Thus, benzene does not order at room temperature on Pd and Pt(111) surfaces, and only weakly on Rh(111). (But coadsorption with CO produces stable ordering through strong interactions between the distinct molecules.)

In the case of weaker chemisorption, such as when CO or NO adsorb intact, there is also relatively little site preference and ordering is less pronounced as well: such molecules choose sites that depend on the metal and on the coverage, as well as on coadsorbates, while low order-disorder transition temperatures are found.

2.5.4.2 CO AND NO ADSORPTION

Detailed structural studies of adsorbed carbon monoxide and nitric oxide have been performed for about 20 surface structures, primarily on close-packed metal surfaces [3]. They have largely confirmed the site assignments based on vibrational frequencies, as originally derived for metal-carbonyl and similar complexes [65], with, however, some notable exceptions at higher coverages. On many metals, CO prefers low-coordination sites at low coverages, e.g. linear coordination at top sites for CO on Rh(111). However, the low-coverage site depends strongly on the metal and the crystallographic face: it is a bridge site on Pd(100) and a 3-fold hollow site on Pd(111).

At higher coverages the coordination generally increases, towards two-fold bridge sites and three-fold hollow sites (but apparently never four-fold hollow sites). The metal-C bond length has been found to increase strongly with coordination, and the C-O bond length increases slightly at the same time [66]. This is again in agreement with the case of metal-carbonyl complexes, and confirms the C-O bond weakening implied by the decreasing vibration frequency.

At high coverages, crowding occurs and part of the CO and NO molecules have to settle for less favorable sites. For instance, at a coverage of 3/4 per cell on Rh(111), one third of the adsorbed CO molecules occupy the favored top sites, while another third occupies 3-fold-coordinated "fcc-hollow" sites, while the remainder bond above "hcp-hollow" sites [67] (the fcc- and hcp-hollow sites differ in that the latter has a metal atom right below this site in the second metal layer, while the former does not). NO in the same circumstances behaves in exactly the same manner [68].

Coadsorption of CO or NO with other adsorbates affects the adsorption site markedly and can lead to dissociation. It is apparent that CO and NO are unusually sensitive monitors of the surface condition. They react strongly to changes in substrate identity, coverage, and coadsorbates. The changes are easily measured, especially through vibrational analysis (HREELS and IRAS).

2.5.4.3 BENZENE ADSORPTION

Benzene adsorbs parallel to fcc(100), fcc(111) and hcp(0001) surfaces, and probably also on other close-packed surfaces [3]. Benzene does not order easily on close-packed metal surfaces, compared to CO, NO and especially atomic adsorbates. At room temperature, benzene does not order at all on Pt and Pd(111), while it weakly orders on Rh(111) (a short exposure to the LEED electron beam is sufficient to destroy the ordered structure).

The adsorption site of benzene is variable, depending on metal, crystallographic face and coadsorbates. It has so far only been determined on fcc(111) and hcp(0001) surfaces [3,69]. On Pt(111), the molecule centers itself over a bridge site, whether benzene is mixed with CO or not [70,71]. On Rh(111), the same site is found for a pure benzene layer, but a 3-fold hollow site emerges in the presence of coadsorbed CO [72]. On Pd(111), in the presence of CO, the 3-fold site is also found [73], while the site is not known for the pure benzene layer. Since the 3-fold hollow site does not exist on other crystal faces, this already implies a change of site in some of these cases.

2.5.5 Adsorbate-induced relaxations

Chemisorption on a surface modifies the chemical environment of the surface atoms and therefore affects the structure. In particular, upon adsorption, any clean-surface relaxation is generally reduced as the surface atoms of the substrate move back towards the ideal bulk-like position or even beyond. Relaxations of deeper interlayer spacings are also usually reduced upon adsorption. In addition, it is becoming increasingly clear that small local distortions on the scale of 0.1 Å are induced around each adsorption site in directions other than the surface normal.

Good examples of the outward relaxation of interlayer spacings are provided by atomic adsorption on the (110) surfaces of nickel and other fcc metals [74]. The clean (110) surfaces typically exhibit contractions by about 10% (0.1 to 0.15 Å) in the topmost interlayer spacing relative to the bulk value. Upon adsorption these contractions are reduced to less than 3 to 4% (0.03 to 0.05 Å).

2.5.6 Adsorbate-induced reconstructions

Adatoms can induce a restructuring of a surface in a variety of ways [74,75]. A mild form of reconstruction occurs when substrate atoms are displaced by small amounts in different directions, thereby changing the unit cell of the substrate (displacive reconstruction). An opposite situation is the removal of a clean-surface reconstruction by an adatom. Also possible is the change from one reconstruction to another. Adatoms can furthermore give rise to new compound formation, or can change surface segregation in an existing compound. On a larger scale, adatoms have also been found to cause macroscopic reshaping of surfaces.

The energy needed for surface restructuring is paid for by the increased bond energies between the adsorbed atom and the substrate. Therefore, such surface restructuring is expected only upon chemisorption where the adsorbate-substrate bond energies are similar to or larger than the bond energies between the atoms in the substrate. This is clearly the case for the adsorption of carbon, oxygen, and sulfur on many transition metals.

2.5.6.1 DISPLACIVE LOCAL RECONSTRUCTION INDUCED BY ADSORPTION}

The adsorption of atoms may displace substrate atoms to provide better adsorbate-substrate bonding, in such a way that a new unit cell results in the substrate [34]. This is a generalization of the adsorbate-induced relaxations discussed above. The local displacements are of the same order of magnitude, at most a few tenths of Å.

The effect is well illustrated with the structure induced by carbon or nitrogen adsorbed on Ni(100) [45,46,47], also seen with O on Rh(100) [76]. The adatom occupies a four-fold site, which it expands by pushing the four neighboring metal atoms outward from the site, parallel to the surface. This allows the adatom to penetrate deeper into the metal surface and to bond not only to the four first-layer metal atoms but also to a metal atom in the next layer. The surrounding metal lattice cannot accept a corresponding compression at a coverage of 0.5 per cell and instead forces a rotation of the square of four metal atoms about the surface normal. Thereby, the average metal density in the top layer is kept constant, while accommodating the additional foreign stoms.

2.5.6.2 REMOVAL OF RECONSTRUCTION BY ADSORPTION

The chemisorption of atoms frequently removes surface reconstruction and produces a more bulk-like surface structure.

Examples of this effect are offered by the removal with hydrogen of the reconstruction of clean Si(100), Si(111) and diamond C(111), and the removal with carbon, oxygen or CO of the reconstructions of the (100) and (110) faces of Ir and Pt. Electron acceptors, like O and S, are particularly effective at removing reconstructions. Sometimes small amounts of adsorbate suffice to remove a reconstruction, but more frequently amounts comparable to a monolayer are required. Hydrogen has to be adsorbed to a coverage of 2 per cell to remove the W(100)-c(2x2) reconstruction [77].

2.5.6.3 CREATION OF RECONSTRUCTION BY ADSORPTION

Adsorbates have frequently been found to induce new reconstructions on surfaces that were not reconstructed in the clean state [74]. Often a small fraction of a monolayer suffices to make the entire surface reconstruct.

Electron donors, like alkali metals, are particularly well known to induce reconstructions on metal surfaces. For example, a small coverage (below 0.1 per cell) of disordered alkali adatoms is sufficient to cause reconstruction of the Ni [78], Cu [79], Pd [80], and Ag(110) [81] surfaces, which transform to the (1x2) missing-row structure. Cs adsorbed on the (1x2) reconstruction of Au(110) causes a (1x3) structure, with only about 5% coverage per cell [82]. This structure is also of the missing-row type, but with deeper troughs than the clean (1x2) structure. A likely reason for this is that large alkali atoms bond more strongly (thanks to more near neighbors) within the deep troughs of the missing rows than in the shallow troughs of the ideal (110) surface [83,84].

Another good example is given by Li or Na adsorbed on Cu(100) or Ni(100) [85]. This forms a series of complex reconstructions that involve a mix of both substitutional adsorption within the top substrate layer and overlayer adsorption above that layer.

More generally, electron-donating adsorbates tend to stabilize metal reconstructions. Stabilization is exemplified by alkali adsorption on the hexagonal reconstruction of Ir(100) [86]. There the clean-surface reconstruction is maintained in the presence of alkali atoms.

2.5.6.4 CHANGE OF RECONSTRUCTION BY ADSORPTION

It stands to reason that surfaces which are already reconstructed when clean are particularly prone to further reconstruction in the presence of adsorbates. This is especially apparent with semiconductor surfaces.

Numerous examples exist where adatoms change the reconstruction of semiconductor surfaces. However, the number of resulting structures which have been solved is relatively small. They concern mostly metal adatoms, such as Al, Ga, and Pb deposited on Si and Ge(111) [52,49,53]. The substrate lattice relaxes noticeably around the adsorption site, with displacements up to about 0.3 Å. Larger adatoms induce larger displacements. The relaxation is noticeable down to the second double layer, which is strongly buckled.

2.5.7 Compound formation and surface segregation

In compound formation from adsorption, a reconstruction occurs that resembles a bulk compound. Continued addition of adsorbate atoms may enable the formation of a thicker film with the three-dimensional lattice of a bulk compound. Such behavior is characteristic of oxidation, nitridation, carbide formation and alloying of metal surfaces. Questions of interest include whether the compound is ordered and, if so, which is the crystallographic orientation of the growing compound. Also the question of lattice matching is important: most growing compounds have a lattice which is mismatched to the substrate [74].

The initial oxidation step of a metal typically involves oxygen atoms nestling between metallic surface atoms. For example, on Ta(100) a submonolayer amount of oxygen takes interstitial positions between the first and second metal layers [87]. An intermediate nitridation step which has been observed consists of the penetration of one monolayer's worth of N atoms between the first and second metal layers of Ti(0001) [88]; the same happens for N adsorbed on Zr(0001) [89].

S on Ni(111) has been observed to form a compound monolayer of composition Ni_2S [90]. It is suggested to have a square lattice of Ni atoms, with every other hollow site occupied by S atoms in a c(2x2) array. This monolayer would lie on the Ni(111) substrate with a (5√3x2)rect coincidence superstructure [91].

Metal silicide compounds are commonly formed after adsorption of metal atoms onto silicon surfaces. Thus, upon Ni deposition on Si(111), $NiSi_2$ grows with its (111) surface interfaced to the substrate [61]. Cobalt [62] and other transition metals behave similarly. For example, Al forms a substitutional GaAsAl compound after deposition on GaAs(110) [54].

Adsorbates may induce large changes of surface composition in multicomponent systems. i.e. surface segregation [74]. Such changes involve atomic diffusion perpendicular to the surface, and thus bond breaking and rebonding. This occurs particularly when the chemisorption bond energies between the alloy components are very different.

One example is the behavior of the Ag-Pd alloy [92]. The clean surface of a Ag-Pd alloy is enriched in silver at any bulk composition because of the lower surface energy of Ag as compared to Pd. Upon adsorption of CO, the surface composition changes rapidly. Because of the greater strength of the Pd-CO bond as compared to the Ag-CO bond, the Pd atoms move to the surface and the alloy surface becomes enriched in Pd. Upon heating CO desorbs and the surface excess of Ag is reestablished.

Acknowledgement

This work was supported by the Director, Office of Science, Office of Basic Energy Sciences, Materials Sciences Division of the U.S. Department of Energy under Contract No. DE-AC03-76SF00098.

References

1. A. Zangwill, *Physics at Surfaces*, Cambridge Univ. Press, Cambridge, 1988.

2. G.A. Somorjai, *Chemistry in Two Dimensions*, Cornell University Press, Ithaca, 1981.

3. P.R. Watson, M.A. Van Hove and K. Hermann, *NIST Surface Structure Database Ver. 4.0*, NIST Standard Reference Data Program, Gaithersburg, 2002.

4. M.A. Van Hove, *Surf. Interface Anal.* 1999, *28*, 36.

5. J.B. Pendry, *Low-Energy Electron Diffraction: The Theory and its Application to Determination of Surface Structure*, Academic Press, London, 1974.

6. M.A. Van Hove, W.H. Weinberg, C.-M. Chan, *Low-Energy Electron Diffraction: Experiment, Theory, and Structural Determination*, Springer-Verlag, Heidelberg, 1986.

7. R. Feidenhans'l, *Surf. Sci. Rep.* 1989, *10*, 105.

8. P.L. Cowan, J.A. Golovchenko, M.F. Robbins, Phys. Rev. Lett. 1980, 44, 1680.

9. C.S. Fadley, in *Synchrotron Research: Advances in Surface Science*, Ed. R.Z. Bachrach, Plenum, New York, 1993.

10. C.S. Fadley, Y. Chen, R.E. Couch, H. Daimon, R. Denecke, H. Galloway, Z. Hussain, A.P. Kaduwela, Y.J. Kim, P.M. Len, J. Liesegang, J. Menchero, J. Morais, J. Palomares, S.D. Ruebush, S. Ryce, M.B. Salmeron, W. Schattke, S. Thevuthasan, E.D. Tober, M.A. Van Hove, Z. Wang, R.X. Ynzunza and J.J. Zaninovich, *J. Surf. Anal.* 1997, *3*, 334.

11. D.P. Woodruff and A.M. Bradshaw, *Rep. Prog. Phys.* 1994, *57*, 1029.

12. See various articles in: *X-ray Absorption: Principles, Applications, Techniques of EXAFS, SEXAFS, and XANES*, Eds. D.C. Koningsberger and R. Prins, Wiley, New York, 1988.

13. J.E. Rowe, in *Synchrotron Research: Advances in Surface Science*, Ed. R.Z. Bachrach, Plenum, New York, 1993.

14. J. Stöhr, *NEXAFS Spectroscopy*, Springer-Verlag, Berlin, Heidelberg, New York, 1992.

15S5. B. Ravel and J.J. Rehr, *J. de Physique* 1997, *IV 7 (NC2)*, 229.

16. J.J. Barton, *Phys. Rev. Lett.* 1988, *61*, 1356.

17. D.K. Saldin, P.L. de Andres, *Phys. Rev. Lett.* 1990, *64*, 1270.

18. M. Aono, Y. Hou, C. Oshima and Y. Ishizawa, *Phys. Rev. Lett.* 1982, *49*, 567.

19. H. Niehus and G. Comsa, *Surf. Sci.* 1984, *140*, 18.

20. J.F. van der Veen, *Surf. Sci. Rep.* 1985, *5*, 199.

21. H. Niehus, G. Comsa, *Surf. Sci.* 1984, *140*, 18.

22. J.F. van der Veen, *Surf. Sci. Rep.* 1985, *5*, 199.

23. E.W. Müller, T.T. Tsong, *Field Ion Microscopy*, American Elsevier, New York, 1969.

24. G. Ehrlich, in *The Structure of Surfaces*, Eds. M.A. Van Hove, S.Y. Tong, Springer-Verlag, Heidelberg, 1985, p. 375.

25. H. Kumar Wickramasinghe, *Scanned-Probe Microscopes*, Scientific American, Vol. 261, No. 4, October 1989, p. 98.

26. R. Wiesendanger, *Scanning Probe Microscopy and Spectroscopy: Methods and Applications*, Cambridge Univ. Press, Cambridge, 1994.

27. H. Ohtani, C.-T. Kao, M.A. Van Hove, G.A. Somorjai, *Progr. Surf. Sci.* 1987, *23*, 155.

28. J.F. Van der Veen, B. Pluis, A.W. Denier van der Gon, in *Chemistry and Physics of Solid Surfaces VII*, Eds. R. Vanselow, R. Howe, Springer-Verlag, Heidelberg, 1988.

29. F. Jona, P.M. Marcus, in *The Structure of Surfaces II*, Eds. J.F. van der Veen, M.A. Van Hove, Springer-Verlag, Heidelberg, Berlin, 1988, p. 90.

30. J.W.M. Frenken, F. Huussen, J.F. van der Veen, *Phys. Rev. Lett.* 1987, *58*, 401.

31. Y. Tian, K.W. Lin, F. Jona, *Phys. Rev.* 2000, *B62*, 12844.

32. C.B. Duke, in *Surface Properties of Electronic Materials*, Eds. D.A. King, D.P. Woodruff, Elsevier, Amsterdam, 1988, p. 69.

33. C.B. Duke, in *Reconstruction of Solid Surfaces*, Eds. K. Christman, K. Heinz, Springer-Verlag, Heidelberg, 1991.

34. S. Titmuss, A. Wander and D.A. King, *Chem. Revs.* 1996, *96*, 1291.

35. E.C. Sowa, M.A. Van Hove, D.L. Adams, *Surf. Sci.* 1988, *199*, 174.

36. M.A. Van Hove, R.J. Koestner, P.C. Stair, J.P. Bibérian, L.L. Kesmodel, I. Bartoš, G.A. Somorjai, *Surf. Sci.* 1981, *103*, 189 and 218.

37. K. Takayanagi, Y. Tanishiro, M. Takahashi, S. Takahashi, *J. Vac. Sci. Technol.* 1985, *A3*, 1502.

38. S.Y. Tong, H. Huang, C.M. Wei, W.E. Packard, F.K. Men, G. Glander and M.B. Webb, *J. Vac. Sci. Technol.* 1988, *A6*, 615.

39. S.Y. Tong, W.N. Mei and G. Xu, *J. Vac. Sci. Technol.* 1984, *B2*, 393.

40. R.J. Baird, D.F. Ogletree, M.A. Van Hove, G.A. Somorjai, *Surf. Sci.* 1986, *165*, 345.

41. M. Gierer, M.A. Van Hove, A.I. Goldman, Z. Shen, S.-L. Chang, P.J. Pinhero, C.J. Jenks, J.W. Anderegg, C.-M. Zhang, and P.A. Thiel, *Phys. Rev.* 1998, *B57*, 7628.

42. T. Cai, F. Shi, Z. Shen, M. Gierer, A.I. Goldman, M.J. Kramer, C.J. Jenks, T.A. Lograsso, D.W. Delaney, P.A. Thiel and M.A. Van Hove, *Surf. Sci.* 2001, *495*, 19.

43. A. Ignatiev, J.B. Pendry, T.N. Rhodin, *Phys. Rev. Lett.* 1971, *26*, 189.

44. H.D. Shih, F. Jona, D.W. Jepsen, P.M. Marcus, *Surf. Sci.* 1976, *60*, 445.

45A34. J. Onuferko, D.P. Woodruff, B.W. Holland, *Surf. Sci.* 1979, *87*, 357.

46. Y. Gauthier, R. Baudoing-Savois, K. Heinz and H. Landskron, *Surf. Sci.* 1991, *251/252*, 493.

47. R. Terborg, J.T. Hoeft, M. Polcik, R. Lindsay, O. Schaff, A.M. Bradshaw, R.L. Toomes, N.A. Booth, D.P. Woodruff, E. Rotenberg and J. Denlinger, *Surf. Sci.* 2000, *446*, 301.

48. K.A. Thompson and C.S. Fadley, *Surf. Sci.* 1984, *146*, 281.

49. H. Huang, C.M. Wei, H. Li, B.P. Tonner, S.Y. Tong, *Phys. Rev. Lett.* 1989, *62*, 559.

50. H. Huang, S.Y. Tong, W.S. Yang, H.D. Shih, F. Jona, *Phys. Rev.* 1990, *B42*, 7483.

51. W. Chen, H. Wu, W.K. Ho, B.C. Deng, G. Xu and S.Y. Tong, *Surf. Rev. Lett.* 2000, *7*, 267.

52. A. Kawazu, H. Sakama, *Phys. Rev.* 1988, *B37*, 2704.

53. H. Huang, S.Y. Tong, J. Quinn, F. Jona, *Phys. Rev.* 1990, *B41*, 3276.

54. A. Kahn, J. Carelli, D. Kanani, C.B. Duke, A. Paton, L. Brillson, *J. Vac. Sci. Technol.* 1981, *19*, 331.

55. G.M. Lamble, R.S. Brooks, D.A. King, D. Norman, *Phys. Rev. Lett.* 1988, *61*, 1112.

56. J.H. Van der Merwe, in *Chemistry and Physics of Solid Surfaces V*, Eds. R. Vanselow, R. Howe, Springer-Verlag, Heidelberg, 1984.

57. R.W. Vook, *Int. Metals Rev.* 1982, *27*, 209.

58. R. Ludeke, *J. Vac. Sci. Technol.* 1984, *B2*, 400.

59. S.H. Lu, Z.Q. Wang, D. Tian, Y.S. Li, F. Jona and P.M. Marcus, *Surf. Sci.* 1989, *221*, 35.

60. K. Heinz, S. Mueller and P. Bayer, *Surf. Sci.* 1995, *337*, 723.

61. E. Vlieg, A.E.M.J. Fischer, J.F. Van der Veen, B.N. Dev, G. Materlik, *Surf. Sci.* 1986, *178*, 36.

62. A.E.M.J. Fischer, E. Vlieg, J.F. Van der Veen, M. Clausnitzer, G. Materlik, *Phys. Rev.* 1987, *B36*, 4769.

63. R.J. Koestner, M.A. Van Hove, G.A. Somorjai, *Surf. Sci.* 1982, *121*, 321.

64. R.J. Koestner, M.A. Van Hove, G.A. Somorjai, *J. Phys. Chem.* 1983, *87*, 203.

65. M.R. Albert, J.T. Yates, Jr., *The Surface Scientist's Guide to Organometallic Chemistry*, American Chemical Society, Washington, 1987.

66. H. Ohtani, M.A. Van Hove, G.A. Somorjai, in *The Structure of Surfaces II*, Eds. J.F. van der Veen, M.A. Van Hove, Springer-Verlag, Heidelberg, Berlin, 1988, p. 219.

67. M. Gierer, A. Barbieri, M.A. Van Hove and G.A. Somorjai, *Surf. Sci.* 1997, *391*, 176.

68. I. Zasada, M.A. Van Hove and G.A. Somorjai, *Surf. Sci.* 1998, *418*, L89.

69. D. Menzel, *Surf. Rev. Lett.* 1999, *6*, 835.

70. D.F. Ogletree, M.A. Van Hove, G.A. Somorjai, *Surf. Sci.* 1987, *183*, 1.

71. A. Wander, G. Held, R.Q. Hwang, G.S. Blackman, M.L. Xu, P. de Andres, M.A. Van Hove and G.A. Somorjai, *Surf. Sci.* 1991, *249*, 21.

72. A. Barbieri, M.A. Van Hove and G.A. Somorjai, *Surf. Sci.* 1994, *306*, 261.

73. A. Barbieri, M.A. Van Hove and G.A. Somorjai, *Surf. Sci.* 1994, *306*, 261.

74. G.A. Somorjai, M.A. Van Hove, Progr. *Surf. Sci.* 1989, *30*, 201.

75. M.A. Van Hove, K. Hermann and P.R. Watson, Landolt-Börnstein, Ed. H. Bonzel, Vol. III/42, Part 1, Chapter 4.1, 2002, in print.

76. J.B. Pendry and K. Heinz, *Surf. Sci.* 1990, *230*, 137.

77. M.A. Passler, B.W. Lee, A. Ignatiev, *Surf. Sci.* 1985, *150*, 263.

78. R.J. Behm, D.K. Flynn, K.D. Jamison, G. Ertl, P.A. Thiel, *Phys. Rev.* 1987, *B36*, 9267.

79. M. Copel, W.R. Graham, T. Gustafsson, S. Yalisove, *Sol. St. Comm.* 1985, *54*, 695.

80. C.J. Barnes, M.Q. Ding, M. Lindroos, R.D. Diehl, D.A. King, *Surf. Sci.* 1985, *162*, 59.

81. B.E. Hayden, K.C. Prince, P.J. Davie, G. Paolucci, A.M. Bradshaw, *Sol. St. Comm.* 1983, *48*, 325.

82. P. Haeberle, T. Gustafsson, *Phys. Rev.* 1989, *B39*, 5810.

83. R.J. Behm, D.K. Flynn, K.D. Jamison, G. Ertl, P.A. Thiel, *Phys. Rev.* 1987, *B36*, 9267.

84. K.W. Jacobsen, J. Nørskov, *Phys. Rev. Lett.* 1988, *60*, 2496.

85. H. Tochihara and S. Mizuno, *Progr. Surf. Sci.* 1998, *58*, 1.

86. K. Heinz, H. Hertrich, L. Hammer, K. Müller, *Surface Sci.* 1985, *152/153*, 303.

87. A.V. Titov, H. Jagodzinski, *Surf. Sci.* 1985, *152/153*, 409.

88. H.D. Shih, F. Jona, D.W. Jepsen, P.M. Marcus, *Surf. Sci.* 1976, *60*, 445.

89. P.C. Wong and K.A.R. Mitchell, *Surf. Sci.* 1987, *187*, L599

90. Y. Kitajima, T. Yokoyama, T. Ohta, M. Funabashi, N. Kosugi and H. Kuroda, *Surf. Sci.* 1989, *214*, L261.

91. J. Luedecke, A.R.H.F. Ettema, S.M. Driver, G. Scragg, M. Kerkar, D.P. Woodruff, B.C.C. Cowie, R.G. Jones and S. Bastow, *Surf. Sci.* 1996, *366*, 260.

92. R. Bouwman, G.H.M. Lippits, W.M.H. Sachtler, *J. Catal.* 1972, *25*, 350.

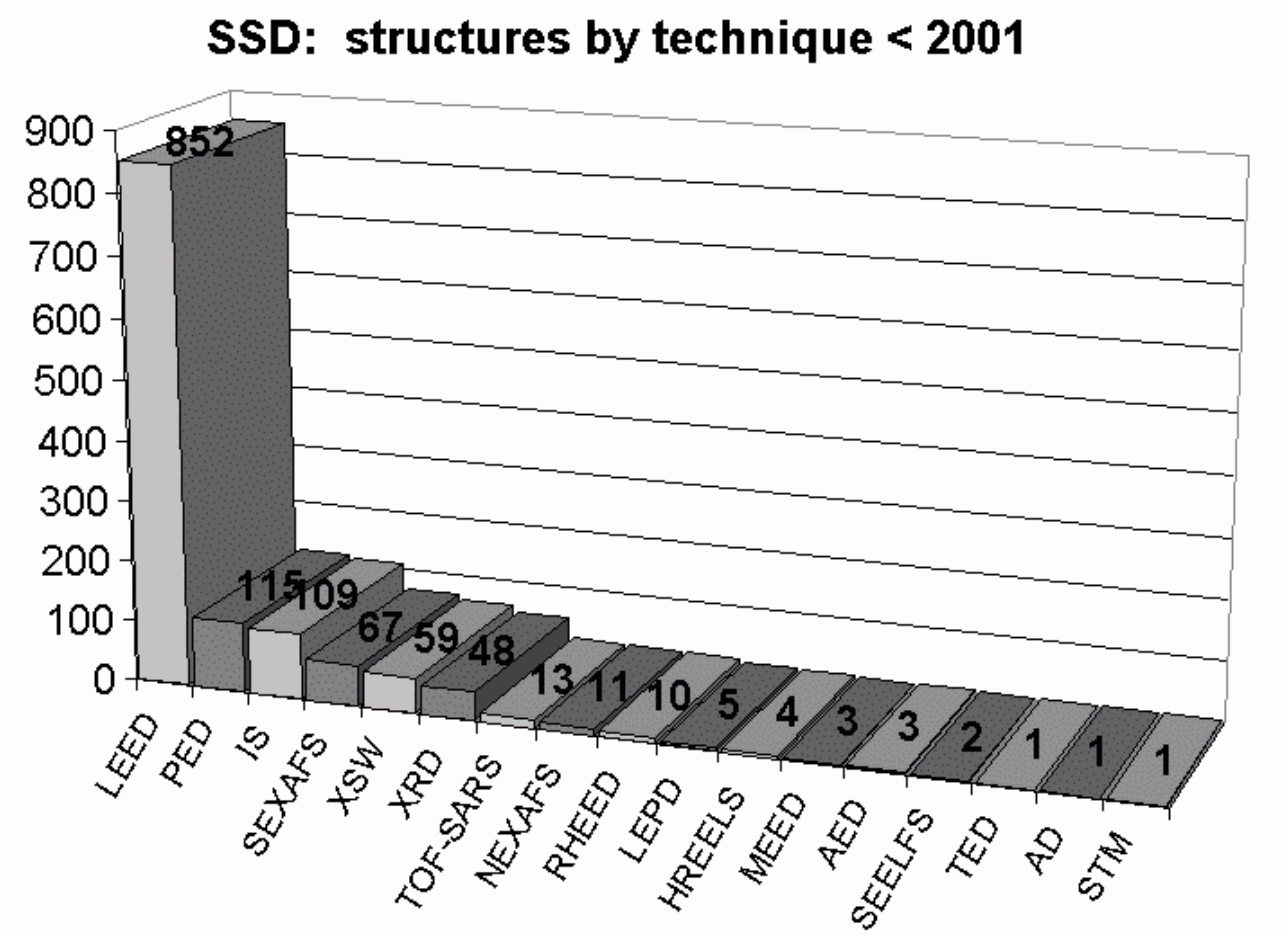

Figure 1. Graph of solved surface structures [from ref. 3], showing the number of structures solved by different techniques through the year 2000. To be included in this graph a technique must have solved structures accurately and completely. As an example, STM had solved only one structure in detail, by comparing STM images to STM theory.

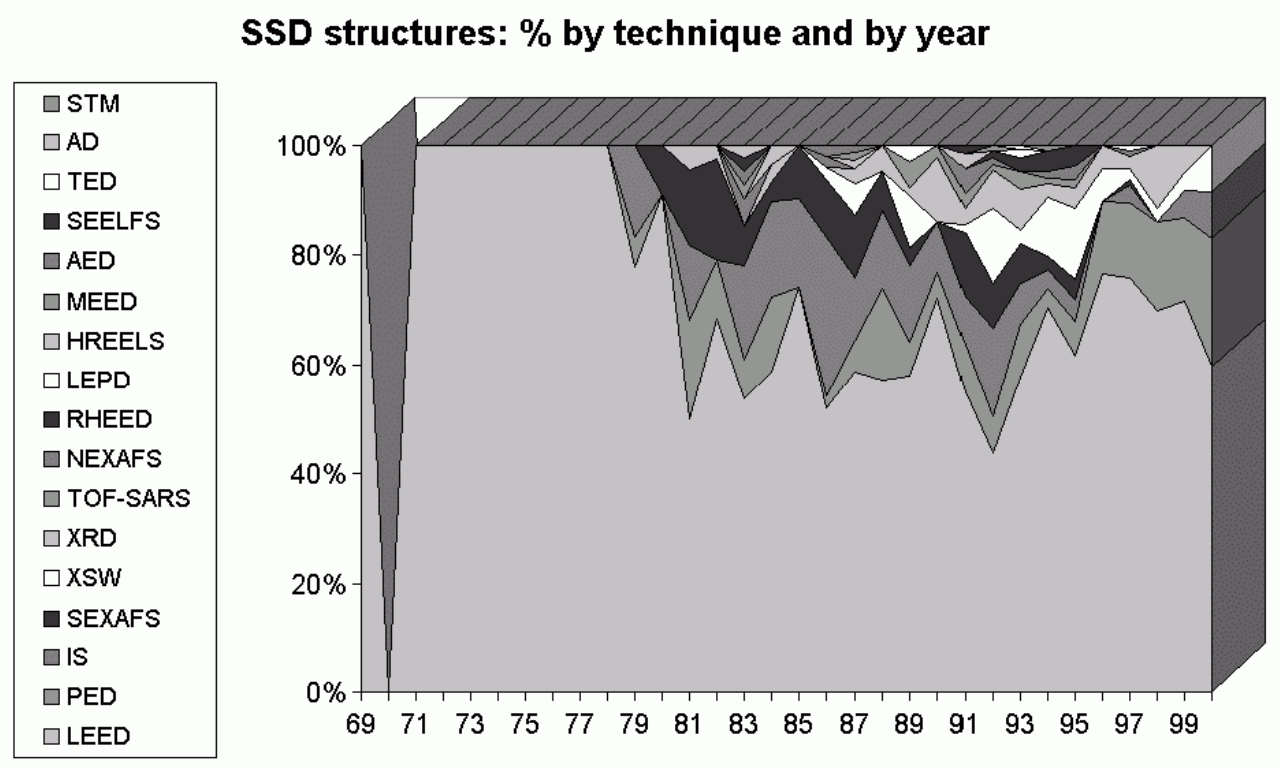

Figure 2. Graph of solved surface structures [from ref. 3], showing year by year the relative contributions from different techniques (no structure was determined in 1970). The techniques are labeled and drawn from bottom up in order of increasing number of structures determined.

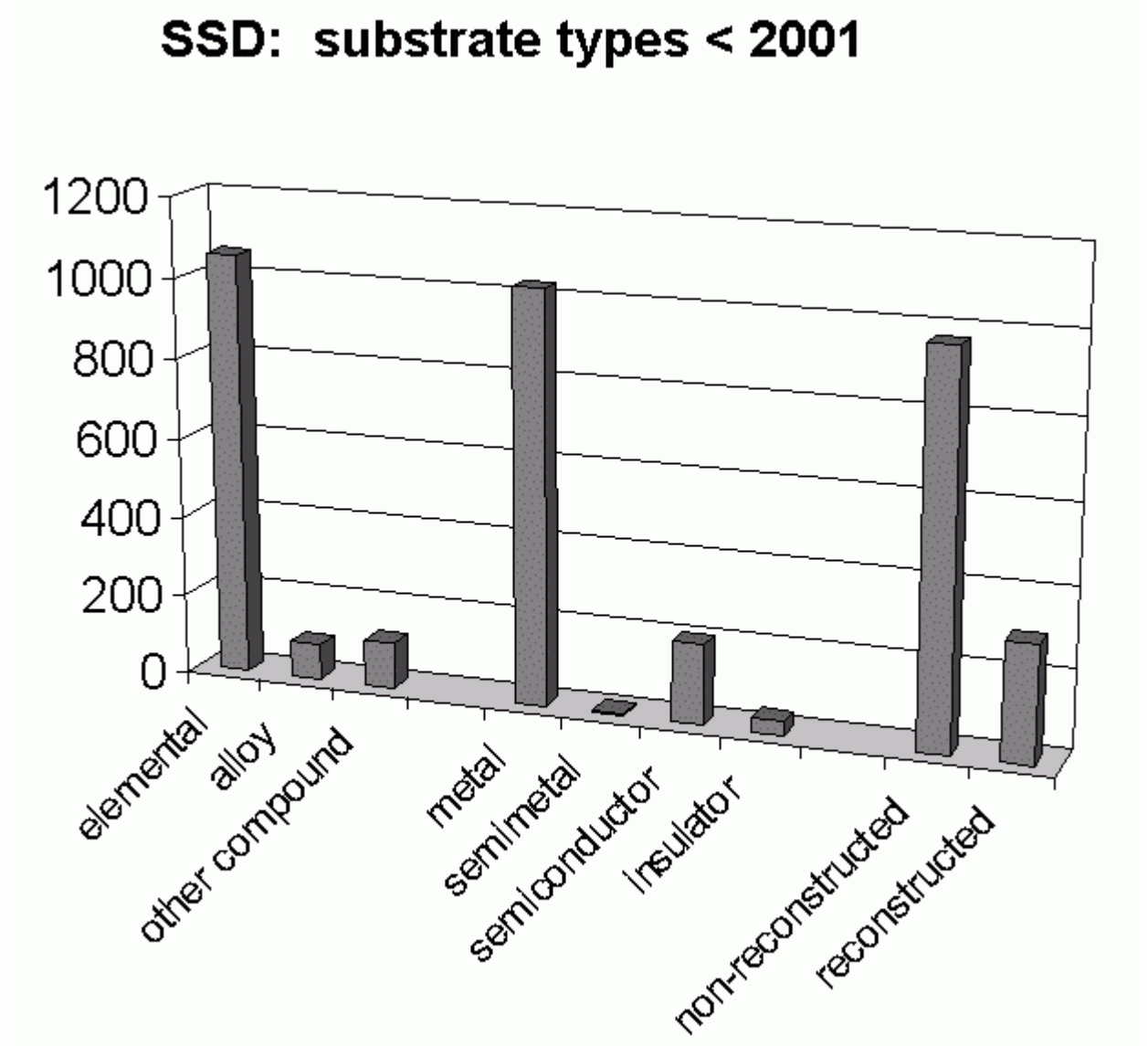

Figure 3. Numbers of solved surface structures classified by types of substrate, through the year 2000 [from ref. 3]. These numbers include both clean and adsorbate-covered surfaces.

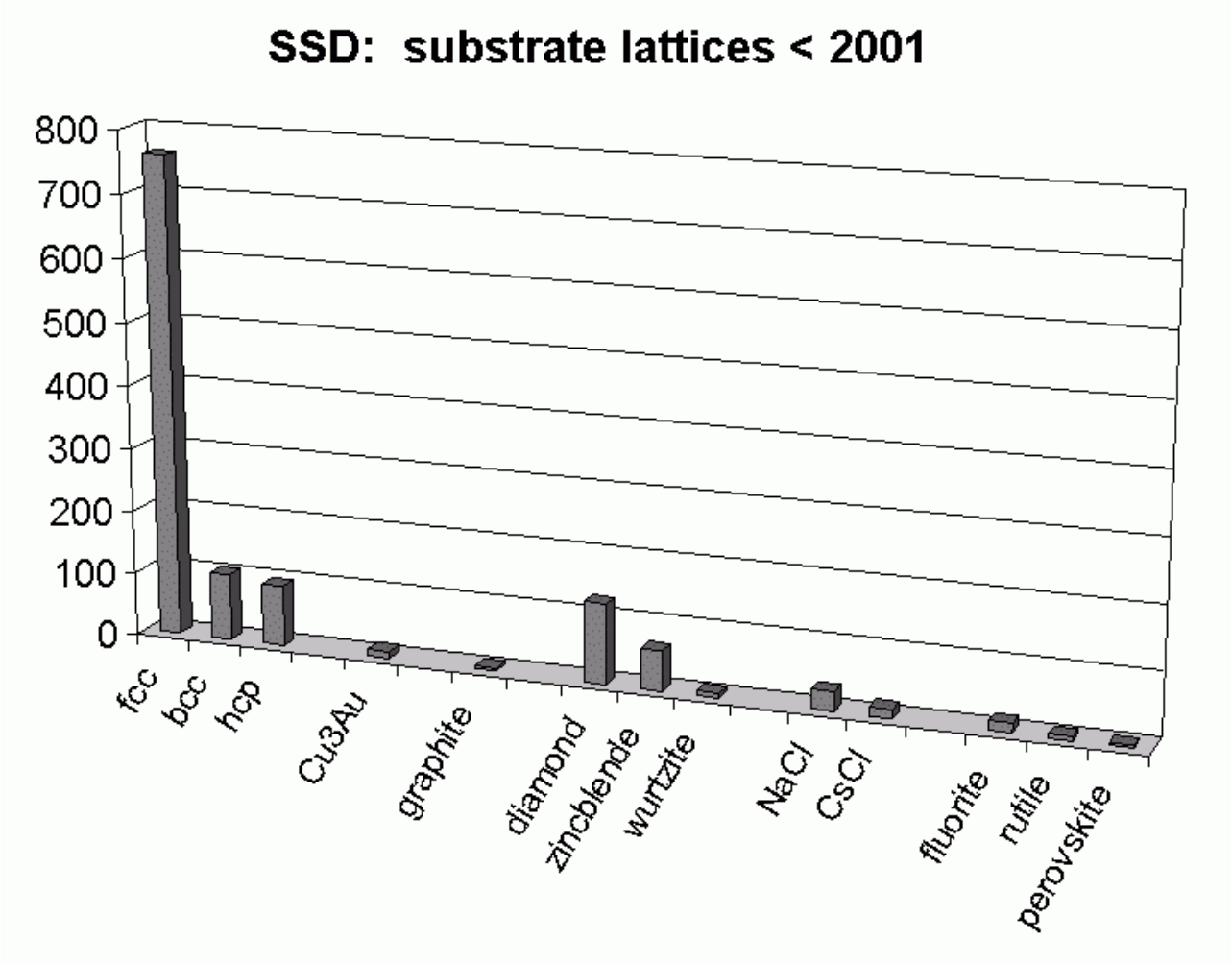

Figure 4. Numbers of solved surface structures classified by substrate lattice, through the year 2000 [from ref. 3]. These numbers include both clean and adsorbate-covered surfaces.

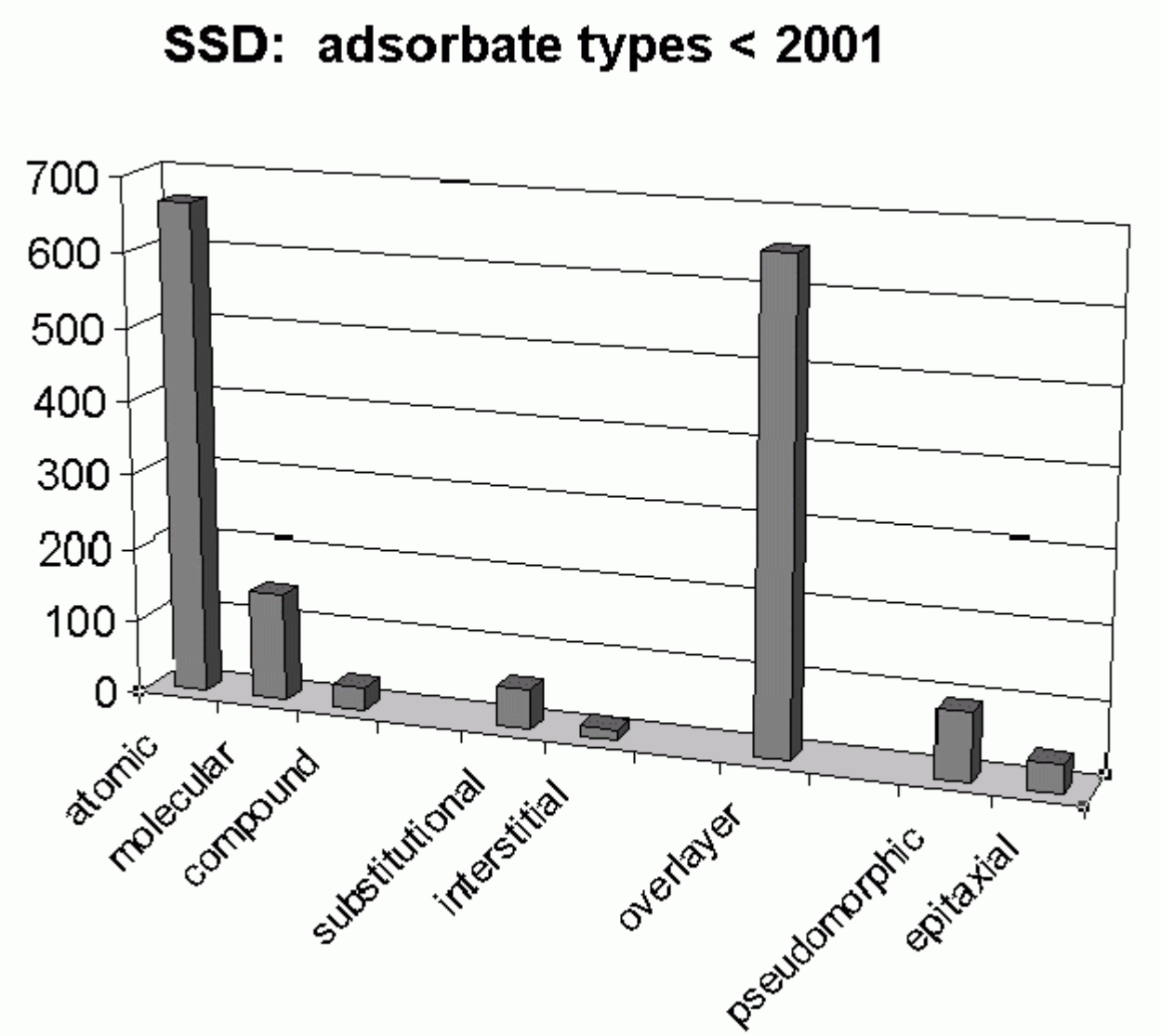

Figure 5. Numbers of solved surface structures classified by type of adsorption, through the year 2000 [from ref. 3].